Yuan *et al. Molecular Cancer* (2026) 25:76
https://doi.org/10.1186/s12943-025-02540-2

Molecular Cancer

RESEARCH Open Access

tRNA m^2G methyltransferase complex THUMPD3-TRMT112 promotes pancreatic cancer progression and autophagy via modulating TFEB translation

Wenbin Yuan[1,2], Shi Li[1], Yue Xi[1], Rui Tian[1], Yuan Liu[1], Xingyu Chen[1], Rui Zhang[1], Hao Lyu[1], Shuai Xiao[1], Dong Guo[1], Qi Zhang[1], Wenying Qin[1], Chaojun Yan[1], Xing-Zhen Chen[3], Cefan Zhou[1*] and Jingfeng Tang[1*]

Abstract

Pancreatic cancer exhibits a heightened level of autophagy, which supports the survival of cancer cells within the malignant microenvironment. The THUMP domain-containing protein 3 (THUMPD3)/ tRNA Methyltransferase Activator Subunit 11–2 (TRMT112) complex has been identified as a tRNA m^2G methyltransferase in mammalian cells, and its functional role remains largely unexplored in pancreatic cancer. In this study, we demonstrate that both THUMPD3 and TRMT112 are upregulated in pancreatic cancer and significantly correlate with poor prognosis for patients. Knockdown of THUMPD3/TRMT112 inhibited pancreatic cancer cell growth in *vitro* and in *vivo*. Additionally, THUMPD3/TRMT112 knockdown significantly reduced autophagic flux, suggesting a role for THUMPD3/TRMT112-mediated tRNA m^2G modification in promoting pancreatic cancer cell proliferation and maintaining autophagy. Mechanistically, THUMPD3/TRMT112 deficiency suppressed TFEB translation via impaired m^2G modification of $tRNA^{Leu(CAG)}$, thereby inhibiting pancreatic cancer cell growth and autophagy. In summary, this study has unveiled the crucial role of the THUMPD3/TRMT112 m^2G tRNA methyltransferase complex in maintaining pancreatic cancer cell growth and autophagy, presenting a promising target for future precision medicine interventions.

Keywords Pancreatic cancer, Autophagy, N2-methylguanosine(m^2G), TRNA, TFEB

*Correspondence:
Cefan Zhou
cefan@hbut.edu.cn
Jingfeng Tang
Jingfeng_hut@163.com
[1]National "111" Center for Cellular Regulation and Molecular Pharmaceutics, Key Laboratory of Fermentation Engineering (Ministry of Education), Cooperative Innovation Center of Industrial Fermentation (Ministry of Education & Hubei Province), Hubei Key Laboratory of Industrial Microbiology, School of Life and Health Sciences, Hubei University of Technology, Wuhan 430068, P. R. China
[2]Hubei Provincial Key Laboratory of Occurrence and Intervention of Kidney Diseases, Hubei Provincial Engineering Research Center of Immunotherapy Drugs for Renal Tumors, College of Medicine, Hubei Polytechnic University, 435003, Huangshi, P. R. China
[3]Membrane Protein Disease Research Group, Department of Physiology, Faculty of Medicine and Dentistry, University of Alberta, Edmonton, AB, Canada

Introduction

Pancreatic cancer is one of the most lethal malignancies, with an exceptionally poor prognosis and a persistently low 5-year survival rate of approximately 5% [1–3]. Given these challenges, elucidating the molecular mechanisms underlying pancreatic cancer and identifying effective therapeutic targets remain urgent priorities [1–3]. Given these challenges, elucidating the molecular mechanisms underlying pancreatic cancer and identifying effective therapeutic targets remain urgent priorities.

Macroautophagy/Autophagy is a health-promoting process wherein misfolded proteins and damaged organelles are sequestered, encapsulated into vesicles, and delivered to lysosomes for degradation via autolysosome formation [4]. Autophagy also serves as an intrinsic survival mechanism for cancer cells, helping them respond to the complex in vivo environment and playing a pivotal role in tumorigenesis [4, 5]. Pancreatic cancer cells exhibit highly active autophagy, which is believed to aid their survival in the harsh tumor microenvironment and facilitate their spread [6].Transcription Factor EB (TFEB) is a central regulator of autophagy, functioning as a master transcription factor that controls lysosomal biogenesis and autophagy. TFEB orchestrates the expression of autophagy and lysosome-related genes, thereby maintaining proteostasis and supporting metabolic adaptation [7]. To exert its transcriptional function, TFEB must translocate into the nucleus, a process that is tightly regulated by phosphorylation. Under nutrient-rich conditions, TFEB remains phosphorylated and sequestered in the cytoplasm, whereas under stress or starvation, dephosphorylation promotes its nuclear import and subsequent activation of autophagy-related gene expression [7, 8]. In pancreatic cancer, TFEB is frequently overexpressed and hyperactivated, which drives the elevated autophagic flux characteristic of pancreatic tumors [9–11]. By promoting proteostasis and enhancing metabolic flexibility, TFEB enables pancreatic cancer cells to adapt to hypoxia and nutrient deprivation in the tumor microenvironment, ultimately facilitating tumor survival, progression, and therapeutic resistance [12]. Autophagy inhibition has been shown to enhance the susceptibility of pancreatic cancer cells to gemcitabine and impair their survival [13]. a phase II clinical trial demonstrated that the autophagy inhibitor hydroxychloroquine (HCQ), combined with gemcitabine or nab-paclitaxel, significantly improved tumor chemosensitivity in patients with pancreatic cancer, potentially creating a window of opportunity for surgical intervention, although no overall survival benefit was observed [4, 14]. However, the efficacy of existing inhibitors remains limited, highlighting the need for novel strategies. Targeting transcription factor EB (TFEB), a master regulator of autophagy, has emerged as a promising approach. Recent studies have revealed that the FDA-approved drug Eltrombopag directly binds to TFEB, inhibits its transcriptional activity, and effectively blocks autophagy, presenting a new direction for enhancing therapeutic sensitivity in pancreatic cancer and other malignancies [15].

Transfer RNAs (tRNAs) are indispensable for protein synthesis, and their modifications critically influence translational fidelity and efficiency. Dysregulated tRNA modifications have emerged as important regulators of cancer biology, impacting tumorigenesis, progression, and metastasis [16–19]. Recent studies have revealed a strong association between dysregulated tRNA modification and various diseases, including cancer [20]. Among them, N2-methylguanosine (m^2G) is one of the common modifications of tRNA [21]. Although the presence of m^2G modification in tRNA is absent in fungi or most bacteria, it is widely observed in human cells and has been found to be regulated by THUMP domain-containing protein 3 (THUMPD3) [22, 23]. Moreover, Loss of THUMPD3 impairs global translation and cell proliferation [23]. tRNA Methyltransferase Activator Subunit 11–2 (TRMT112), a highly conserved small protein lacking an methyltransferases (MTase) catalytic domain, serves as an essential cofactor and activator for various MTases involved in the methylation of rRNA, tRNA, and proteins [24]. The TRMT112 not only enhances the SAM binding affinity of THUMPD3, but also potentially contributes to the stabilization of THUMPD3 by concealing hydrophobic regions [23]. Recent findings have demonstrated a lack of proportional correlation between protein abundance and mRNA abundance in cancer, with certain oncogenes being aberrantly overexpressed through translational mechanisms. The modulation of tRNA modification plays a pivotal role in maintaining protein translation within cancer cells. Furthermore, preliminary evidence suggests that METTL1-mediated m^7G tRNA modification may interfere autophagy via translational regulation [25]. However, the role of tRNA m^2G modification and its associated modifying enzyme THUMPD3-TRMT112 in the proliferation and autophagy of pancreatic cancer remains unexplored.

In this study, we have demonstrated a significant upregulation of THUMPD3 and TRMT112 expression levels in pancreatic cancer patients, strongly correlated with poor prognosis. Depletion of the dysregulated tRNA m^2G methyltransferase complex (THUMPD3-TRMT112) leads to a substantial reduction in m^2G-modified tRNA expression and inhibits autophagic flux, thereby impeding the proliferation and progression of pancreatic cancer cells both in vitro and in vivo. Our findings highlight that THUMPD3-TRMT112-mediated m^2G modification of $tRNA^{Leu(CAG)}$ enhances the translational activity of TFEB, consequently promoting autophagy initiation and survival in pancreatic cancer. This study elucidates

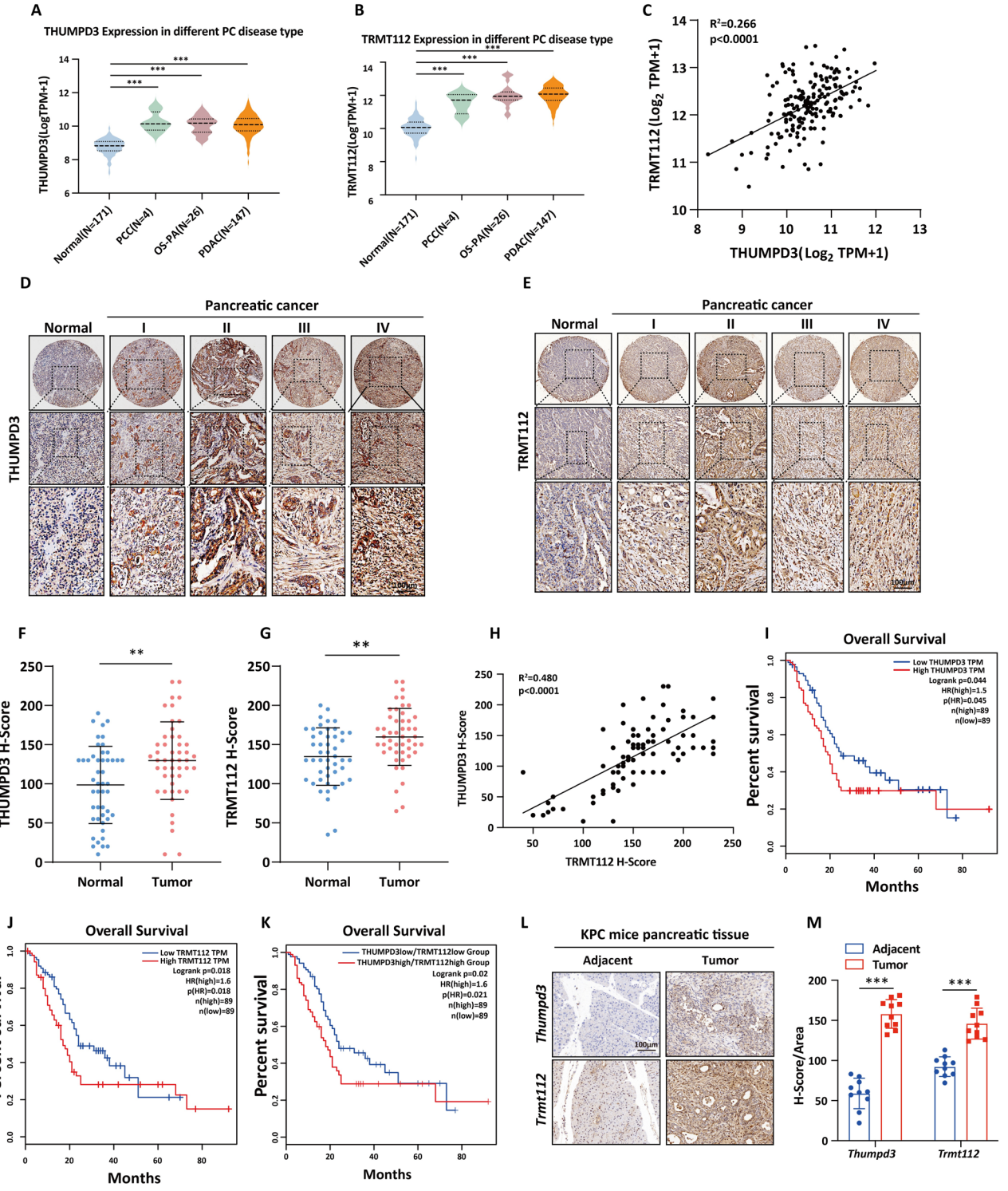

Fig. 1 (See legend on next page.)

the critical link between tRNA m^2G modification and autophagy regulation in pancreatic cancer. Our study identifies THUMPD3-TRMT112 as a regulator of autophagy and proliferation in pancreatic cancer, revealing a tRNA m^2G-dependent pathway that contributes to tumor maintenance. These findings position THUMPD3-TRMT112 as a potential therapeutic target worthy of further investigation, providing new insights for developing intervention strategies against pancreatic cancer.

(See figure on previous page.)

Fig. 1 THUMPD3-TRMT112 is up-regulated in PAADs and is a negative prognostic factor for PAAD patients. **A** Expression of THUMPD3 in different pancreatic cancer disease type(PCC, Pancreas-Colloid Carcinoma; OS-PA, Pancreas-Adenocarcinoma-Other Subtype; PDAC, Pancreas-Adenocarcinoma Ductal Type), data were downloaded from the TCGA-PAAD database. **B** Expression of TRMT112 in different pancreatic cancer disease type, data were downloaded from the TCGA-PAAD database. **C** TRMT112 levels were positively correlated with the levels of THUMPD3 in TCGA PAAD database. **D-G** Representative immunohistochemical images of THUMPD3 and TRMT112 expression in human pancreatic cancer tissues and normal pancreatic tissues and the quantification of THUMPD3 and TRMT112 intensity. **H** TRMT112 levels were positively correlated with the levels of THUMPD3 in human pancreatic cancer tissues and normal pancreatic tissues. **I, J** Kaplan–Meier curves of THUMPD3 and TRMT112 expression in pancreatic adenocarcinoma, data were downloaded from the GEPIA database. **K** Kaplan–Meier survival curves for THUMPD3-TRMT112 expression in pancreatic adenocarcinoma. Survival data were obtained from the GEPIA database and stratified by high vs low gene expression. **L, M** Representative immunohistochemical images of Thumpd3 and Trmt112 expression in KPC mice pancreatic tissues and the quantification of Thumpd3 and Trmt112 intensity (n = 10). *p < 0.05; **p < 0.01; ***p < 0.001. Data were presented as mean ± SD

Result

THUMPD3-TRMT112 is significantly upregulated in pancreatic cancer tissues and associated with poor prognosis

To investigate the expression of THUMPD3 and TRMT112 in pancreatic cancer, we conducted an analysis using the TCGA and GTEx databases. Our analysis revealed significantly elevated levels of THUMPD3 and TRMT112 in various disease subtypes of pancreatic cancer tissues compared to normal tissues (Fig. 1A and B). Furthermore, correlation analysis showed a significant positive correlation between THUMPD3 and TRMT112 expression in pancreatic cancer tissues (Fig. 1C). These findings were further validated in clinical pancreatic cancer specimens(Fig.1 D-H). Importantly, high expression of either THUMPD3 or TRMT112 was associated with significantly poorer overall survival in pancreatic cancer patients (Fig. 1I and J). To further evaluate their combined prognostic value, we performed a two-gene signature analysis using TCGA-PAAD data. Patients stratified into a THUMPD3high/TRMT112high co-expression group exhibited significantly worse overall survival compared to the THUMPD3low/TRMT112low group (Fig. 1K), underscoring the clinical relevance of THUMPD3-TRMT112 complex. At the animal level, we confirmed these observations in the genetically engineered KPC mice model, where THUMPD3 and TRMT112 expression levels were significantly higher and positively correlated in tumor tissues compared to adjacent normal tissues (Fig. 1L and M, Fig. S1A). Additionally, immunohistochemistry in both patient specimens and KPC tumors showed that THUMPD3 and TRMT112 signals were predominantly localized to tumor epithelial cells with weak stromal staining (Fig. 1D, E and L). Collectively, these results establish that THUMPD3 and TRMT112 are consistently overexpressed in pancreatic cancer across human patients and KPC mice models, and associate with poor prognosis, supporting their potential role in pancreatic cancer progression.

THUMPD3-TRMT112 knockdown impaired pancreatic cancer progression

To validate the expression of THUMPD3 and TRMT112 in pancreatic cancer, we examined their levels across a panel of pancreatic cancer cell lines. Notably, PANC-1 and AsPC-1 cells showed substantially higher expression of both THUMPD3 and TRMT112 (Fig. S2A). Based on this finding, we generated stable knockdown cell lines for THUMPD3 and TRMT112 in PANC-1 and AsPC-1 backgrounds (Fig. 2A). Follow-up functional analyses were conducted using specific shRNAs targeting THUMPD3 (shTHUMPD3#1) and TRMT112 (shTRMT112#1). To further clarify the reciprocal decrease of THUMPD3 and TRMT112 observed upon knockdown, cycloheximide chase assays combined with MG132 or chloroquine treatment revealed that both proteins undergo ubiquitin–proteasome pathway mediated degradation rather than autophagy-lysosomal pathway (Fig. S3A). These findings initially indicate that THUMPD3 and TRMT112 co-stabilize each other within the complex.

Depletion of THUMPD3 or TRMT112 significantly inhibited the proliferation of PANC-1 and AsPC-1 cells, as evidenced by MTT assays (Fig. 2B and C). This suppression of proliferation was accompanied by enhanced apoptosis, indicated by increased Annexin V/PI staining and elevated levels of cleaved caspase-3 in vitro (Fig. S4A-C). Supporting bioinformatic analyses implicating THUMPD3 and TRMT112 in proliferation regulation (Fig. S5A and S5B), functional studies confirmed that knockdown of either THUMPD3 or TRMT112 markedly attenuated migration and invasion in Transwell assays (Fig. 2D-H), reduced colony-forming ability (Fig. 2I-K), and delayed wound closure (Fig. S6A-D). Furthermore, EdU incorporation assays demonstrated a significant decrease in DNA synthesis upon THUMPD3 or TRMT112 knockdown (Fig. S6E-H), corroborating the defect in cell proliferation.

To evaluate the role of THUMPD3 and TRMT112 in tumorigenesis in vivo, we employed a xenograft model in BALB/c-nu mice. Knockdown of THUMPD3 or TRMT112 led to a significant reduction in both tumor incidence and tumor weight (Fig. 2L-N). Immunohistochemical analysis of xenograft tissues further revealed a

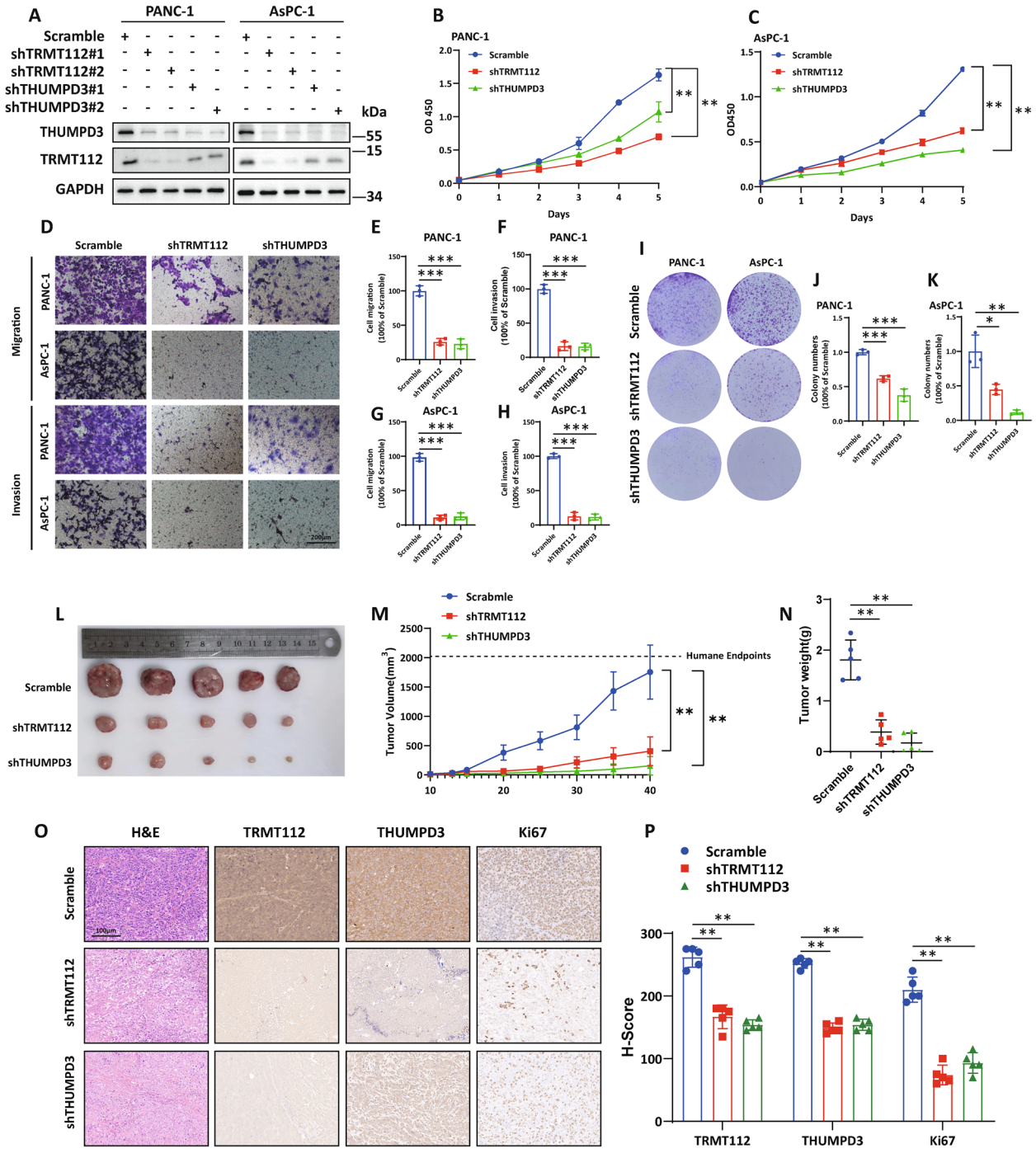

Fig. 2 THUMPD3-TRMT112 inhibition prevented PAAD progression in vitro and in xenograft models. **A** The effect of THUMPD3 and TRMT112 shRNA was detected by WB in PANC-1 and AsPC-1 cell lines. **B-C** MTT assay showed that THUMPD3 and TRMT112 knockdown could reduce the viability of PANC-1 and AsPC-1 cells ($n=5$). **D-H** Representative images and quantification of the transwell assays with or without matrigel of PANC-1 and AsPC-1 cells stably expressed Scramble RNA, THUMPD3 or TRMT112 shRNA ($n=3$). **I-K** Representative images and quantification of the plate colony formation assays of PANC-1 and AsPC-1 cells stably expressed Scramble RNA, THUMPD3 or TRMT112 shRNA ($n=3$). **L** Representative images of excised tumors in different groups injected with PANC-1 cells stably expressed Scramble RNA, THUMPD3 or TRMT112 shRNA of nude mice were shown ($n=5$). **M** Growth curve showing the changes in the tumor volume in mice in different groups from the injection ($n=5$). **N** Weight of the excised tumors in each group ($n=5$). **O** Representative H&E staining images and immunohistochemical images of TRMT112, THUMPD3 and Ki67 expression in excised tumors tissues. **P** The quantification of TRMT112, THUMPD3 and Ki67 expression intensity in excised tumors tissues. $^{*}p<0.05$; $^{**}p<0.01$; $^{***}p<0.001$. Data were presented as mean ± SD

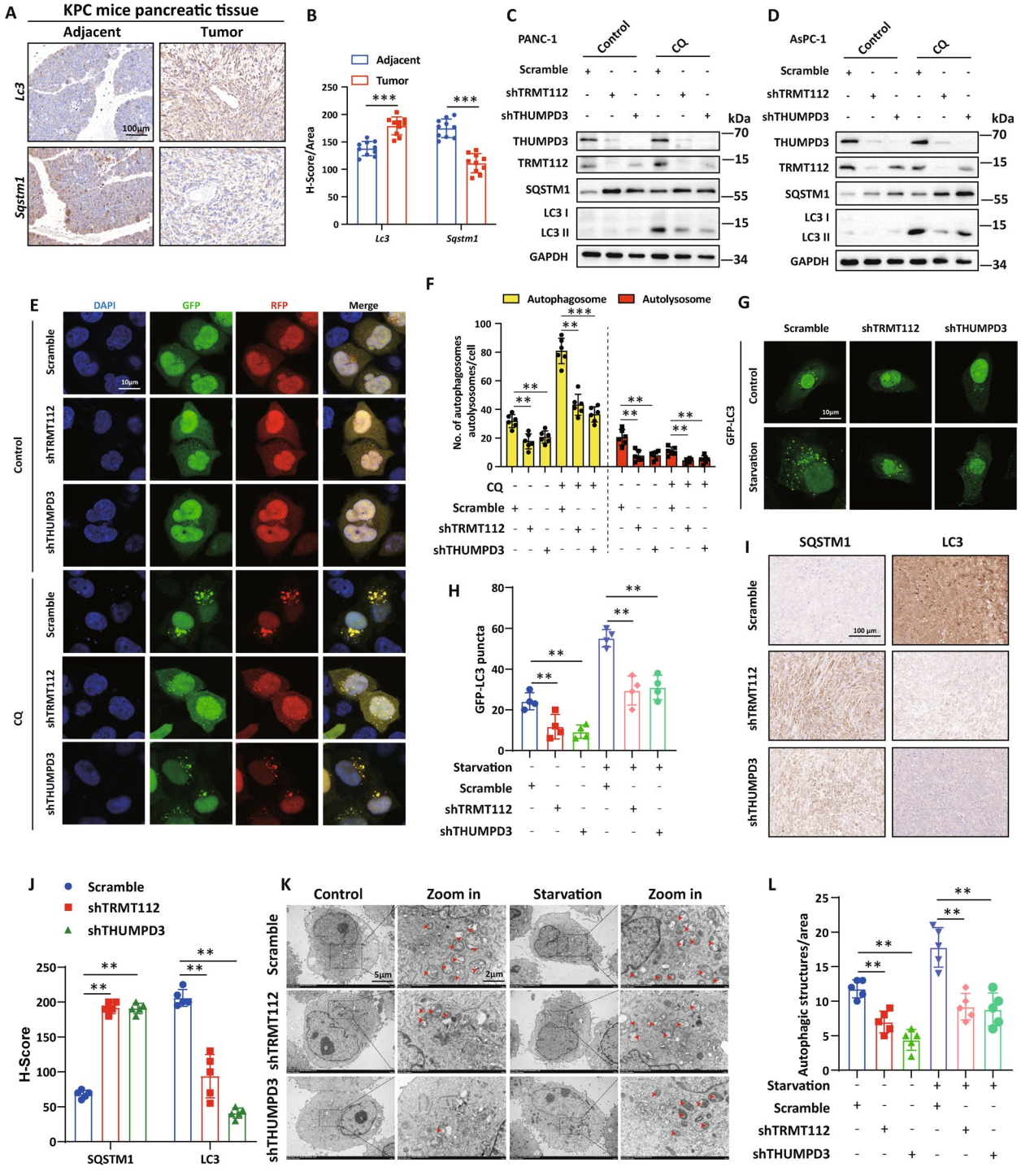

Fig. 3 (See legend on next page.)

pronounced decrease in Ki67-positive cells, along with enhanced cleaved caspase-3 immunostaining in the knockdown groups (Fig. 2O and P, Fig. S4D and S4E). Taken together, these results underscore critical roles for THUMPD3 and TRMT112 in promoting proliferation and tumorigenicity in pancreatic cancer.

Depletion of THUMPD3-TRMT112 impairs autophagy in pancreatic cancer cells

We initially identified THUMPD3 and TRMT112 as potential regulators of autophagy through a preliminary GSEA analysis of the TCGA database (Fig. S7A and S7B). To establish a relevant cellular model, we assessed autophagic flux across pancreatic cell lines and found

(See figure on previous page.)

Fig. 3 Knockdown THUMPD3-TRMT112 impaired autophagy in pancreatic cancer cells. **A**, **B** Representative immunohistochemical images of *Lc3* and *Sqstm1* expression in KPC mice pancreatic tissues and the quantification of *Lc3* and *Sqstm1* intensity ($n=10$). **C**, **D** PANC-1 and AsPC-1 cells were stably expressed with Scramble RNA, THUMPD3 or TRMT112 shRNA; the cells were then treated with or without CQ (20 μM) treatment for another 6 h. Then, the cell lysates were sent to western blotting using indicated antibodies. **E**, **F** Autophagic flux was detected with the mRFP-GFP-LC3 reporters. PANC-1 cells were stably expressed with Scramble RNA, THUMPD3 or TRMT112 shRNA were separately co-transfected with mRFP-GFP-LC3 under with or without CQ (20 μM) treatment. Representative confocal images are shown, and the number of cells showing an accumulation of yellow or red puncta was quantified ($n=6$). **G**, **H** Representative confocal images of GFP-LC3 puncta in the PANC-1 cells were stably expressed with Scramble RNA, THUMPD3 or TRMT112 shRNA were separately co-transfected with GFP-LC3 with or without EBSS conditions. The number of GFP-LC3 puncta was quantified using ImageJ software ($n=4$). **I** Representative immunohistochemical images of SQSTM1 and LC3 expression in excised tumors tissues. **J** The quantification of SQSTM1 and LC3 expression intensity in excised tumors tissues ($n=5$). **K**, **L** Representative electronic micrographs of the autophagosomes or the autolysosomes of the PANC-1 cells were stably expressed with Scramble RNA, THUMPD3 or TRMT112 shRNA with or without EBSS treatment for another 6 h. The number of autophagic structures per area was quantified (n = 5). $^{*}p<0.05$; $^{**}p<0.01$; $^{***}p<0.001$. Data were presented as mean ± SD

that PANC-1, AsPC-1 and BxPC-3 cells exhibited significantly higher basal autophagic activity compared to normal pancreatic ductal cells. Importantly, this subset of autophagy-active cancer cells showed a potential positive correlation between THUMPD3-TRMT112 expression levels and autophagic flux (Fig. S7C, Fig S2A), supporting our selection of PANC-1 and AsPC-1 as representative models for mechanistic investigation. This relationship was further validated in the KPC mouse model, where immunohistochemical analysis demonstrated enhanced autophagic activity in tumor tissues, characterized by increased LC3 and decreased p62 expression, which paralleled the elevated THUMPD3 and TRMT112 levels (Fig. 3A and B, Fig. 1L and M).

Furthermore, western blot analysis revealed a significant accumulation of SQSTM1 upon knockdown of THUMPD3 and TRMT112 in PANC-1 and AsPC-1 cells, while LC3 II accumulation was reduced following treatment with chloroquine (CQ) (Fig. 3C and D). To investigate the impact of THUMPD3 and TRMT112 knockdown on autophagic flux, we employed mRFP-GFP-LC3 tandem reporters to visualize differences between autophagosomes (GFP-positive/RFP-positive, appearing as yellow spots) and autolysosomes (GFP-negative/RFP-positive, appearing as red spots). The results showed a significant reduction in the number of red spots upon depletion of THUMPD3 and TRMT112, as well as a notable decrease in yellow puncta following treatment with CQ (Fig. 3E and F). To evaluate autophagosome formation, we utilized GFP-LC3 immunofluorescence in PANC-1 cells and observed that the number of GFP-LC3 puncta formed under basal and EBSS conditions was significantly reduced upon THUMPD3 and TRMT112 knockdown (Fig. 3G and H). Immunohistochemical analysis of PANC-1 xenograft tumors revealed that knockdown of THUMPD3 and TRMT112 markedly reduced the staining intensity of LC3 while increasing the staining intensity of SQSTM1 (Fig. 3I and J). Transmission electron microscopy provided further evidence, showing a significant reduction in the number of autophagosomes in cells upon knockdown of THUMPD3 and TRMT112 (Fig. 3K and L). Taken together, our data demonstrate that depletion of THUMPD3-TRMT112 impairs autophagy in pancreatic cancer cells, highlighting its crucial role in autophagic regulation. These findings enhance our understanding of the molecular mechanisms underlying autophagy in pancreatic cancer.

THUMPD3-TRMT112 promotes the proliferation of pancreatic cancer cells via autophagy pathway

Further exploring the role of THUMPD3-TRMT112-mediated autophagy activation in pancreatic cancer, we used MTT assays to assess cell proliferation when overexpressing THUMPD3 or TRMT112 with or without CQ treatment (Fig. 4A). The results showed that the overexpression of either THUMPD3 or TRMT112 significantly enhanced PANC-1 cell proliferation and effectively rescued the inhibition of cell proliferation induced by CQ. We further used a tumor xenograft model by subcutaneous injection of PANC-1 cells stably overexpressing THUMPD3 or TRMT112 or Vector in nude mice, with or without treatment with the autophagy inhibitor CQ at a dosage of 60 mg/kg, which has been previously established in pancreatic cancer xenograft studies to effectively inhibit autophagy while maintaining a favorable safety profile [26] (Fig. 4B). Our findings demonstrated that the overexpression of THUMPD3 and TRMT112 resulted in significantly larger tumor volumes and faster growth rate compared to the Vector group (Fig. 4C-E). Moreover, the enhanced expression of THUMPD3 and TRMT112 effectively counteracted the diminished tumorigenic ability induced by CQ treatment. Consistently, immunohistochemical analysis of tumor tissues revealed that THUMPD3 or TRMT112 overexpression increased the percentage of Ki67-positive cells, elevated LC3 levels, and reduced SQSTM1n levels (Fig. 4F and G). Overall, our findings indicate that THUMPD3 and TRMT112 can promote pancreatic cancer cell proliferation by sustaining autophagic flux, although additional autophagy-independent mechanisms may also contribute to their pro-tumorigenic activity.

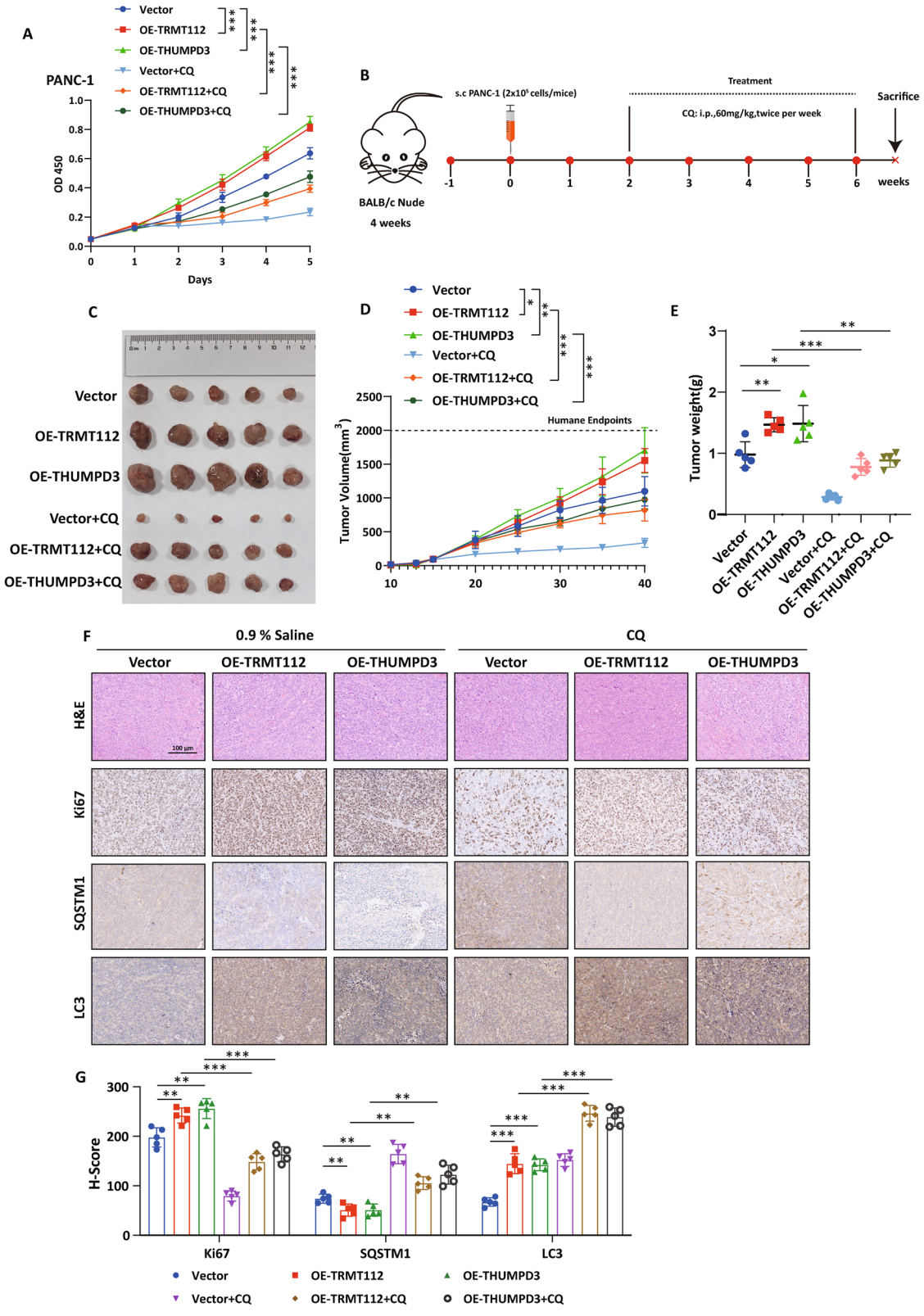

Fig. 4 (See legend on next page.)

(See figure on previous page.)

Fig. 4 THUMPD3-TRMT112 facilitates the proliferation of pancreatic cancer cells via activation of the autophagy pathway. **A** MTT assay for PANC-1 cells were stably expressed TRMT112 or THUMPD3; the cells were then treated with or without CQ (20 μM) treatment for indicated duration ($n = 5$). **B** Schematic diagram of the experimental procedure of the treatment of the CQ to nude mice xenograft formation. **C** Representative images of excised tumors in the groups with respective CQ treatment were shown. **D** The growth curve shows the changes in the tumor volume in mice in different groups ($n = 5$). **E** Weight of the excised tumors in each group ($n = 5$). **F** Representative H&E staining images and immunohistochemical images of Ki67, SQSTM1 and LC3 expression in excised tumors tissues. **G** The quantification of Ki67, SQSTM1 and LC3 expression intensity in excised tumors tissues ($n = 5$). *$p < 0.05$; **$p < 0.01$; ***$p < 0.001$. Data were presented as mean ± SD

THUMPD3-TRMT112 methyltransferase complex is required for the maintenance of pancreatic cancer cell growth and autophagy

The K48 site of TRMT112 has been reported to play a crucial role in facilitating the interaction with THUMPD3 [24]. Consequently, we introduced inactivating mutations at this specific site to elucidate the impact of THUMPD3 binding to TRMT112 on the proliferation of pancreatic cancer cells. Co-immunoprecipitation assays, including both forward and reverse experiments, confirmed that the K48A mutation in TRMT112 significantly attenuated its interaction with THUMPD3 (Fig. 5A and B). Interestingly, immunofluorescence results revealed a cytoplasmic localization of the THUMPD3 and TRMT112 interaction, while TRMT112 demonstrated nuclear distribution when it was mutated (Fig. 5C). To explore the mechanism underlying this localization shift, we performed bioinformatic analysis which indicated that TRMT112 lacks a classical nuclear localization signal (NLS) (Fig. S8A). Moreover, our findings suggest that the nuclear translocation of TRMT112-K48A is not dependent on CRM1 (Fig. S8B and S8C). Based on these data, we propose that the relatively small TRMT112 protein (~15 kDa) is constitutively tethered in the cytoplasm through its high-affinity interaction with THUMPD3, and that disruption of this interaction via the K48A mutation liberates TRMT112, thereby allowing it to passively diffuse into the nucleus where it may be retained by other binding partners.

To independently validate this interaction and its localization, we employed bimolecular fluorescence complementation (BiFC). Venus fluorescent protein fragments (VN 1–155 and VC 156–239) fused to THUMPD3 and TRMT112, respectively, produced a strong cytoplasmic BiFC signal upon interaction, which was markedly reduced by the TRMT112-K48A mutation (Fig. 5D-F), confirming the critical role of the K48 site in complex formation and cytoplasmic retention.

We next examined the functional consequences of disrupting the THUMPD3-TRMT112 complex. While THUMPD3 overexpression promoted PANC-1 cell proliferation, this effect was abolished upon TRMT112 knockdown (Fig. 5G). Rescue experiments demonstrated that re-expression of wild-type TRMT112, but not the K48A mutant, restored migration, invasion (Fig. 5H-J), proliferation (Fig. 5K), and colony formation (Fig. 5L and M) in TRMT112-depleted PANC-1 cells.

The functional integrity of the THUMPD3-TRMT112 complex was also required for autophagy maintenance. Re-expression of TRMT112-WT, but not the K48A mutant, rescued the autophagic blockade caused by TRMT112 knockdown and stabilized THUMPD3 protein levels (Fig. 5N). Moreover, compared to the TRMT112-K48A mutant, TRMT112-WT more effectively promoted the proliferation of PANC-1 cells via autophagy (Fig. 5O). Together, these results demonstrate that TRMT112 exerts both THUMPD3-dependent and THUMPD3-independent biological functions, and that the K48 residue is essential specifically for the autophagy-supporting and cytoplasmic THUMPD3-associated activities of the complex. In summary, these results establish that the direct interaction between TRMT112 and THUMPD3, mediated by the TRMT112 K48 residue, is indispensable for the cytoplasmic localization of the complex, the maintenance of autophagic flux, and the proliferation of pancreatic cancer cells.

TFEB is a potential regulator of THUMPD3-TRMT112-mediated autophagy in pancreatic cancer cells

In order to further elucidate the involvement of the THUMPD3-TRMT112 complex in autophagy, we performed RT-qPCR and western blot analysis to screen for commonly implicated autophagy-related genes (Fig. 6A-C). We observed a widespread suppression of autophagy upon knockdown of THUMPD3 and TRMT112. This coordinated suppression across the autophagy pathway strongly suggested the impairment of a common upstream transcriptional regulator. Based on this evidence, we focused on Transcription Factor EB (TFEB), a master regulator known to coordinately transactivate a broad set of autophagy and lysosomal genes [7]. Interestingly, while immunohistochemical analysis of KPC mice pancreatic tissues demonstrated elevated TFEB expression in tumor areas (Fig. S9A-C), western blot analysis revealed that TFEB protein levels in PANC-1 and AsPC-1 cells were not markedly higher than in the normal pancreatic ductal cell line HPDE6-C7 (Fig. S9D). This suggests that the functional regulation of TFEB in these cancer cells may occur primarily at the post-translational level.

To validate this hypothesis, we demonstrated that TFEB restoration rescues both the autophagy inhibition (Fig. 6D) and lysosomal dysfunction (Fig. 6E and F) induced by THUMPD3 or TRMT112 knockdown in

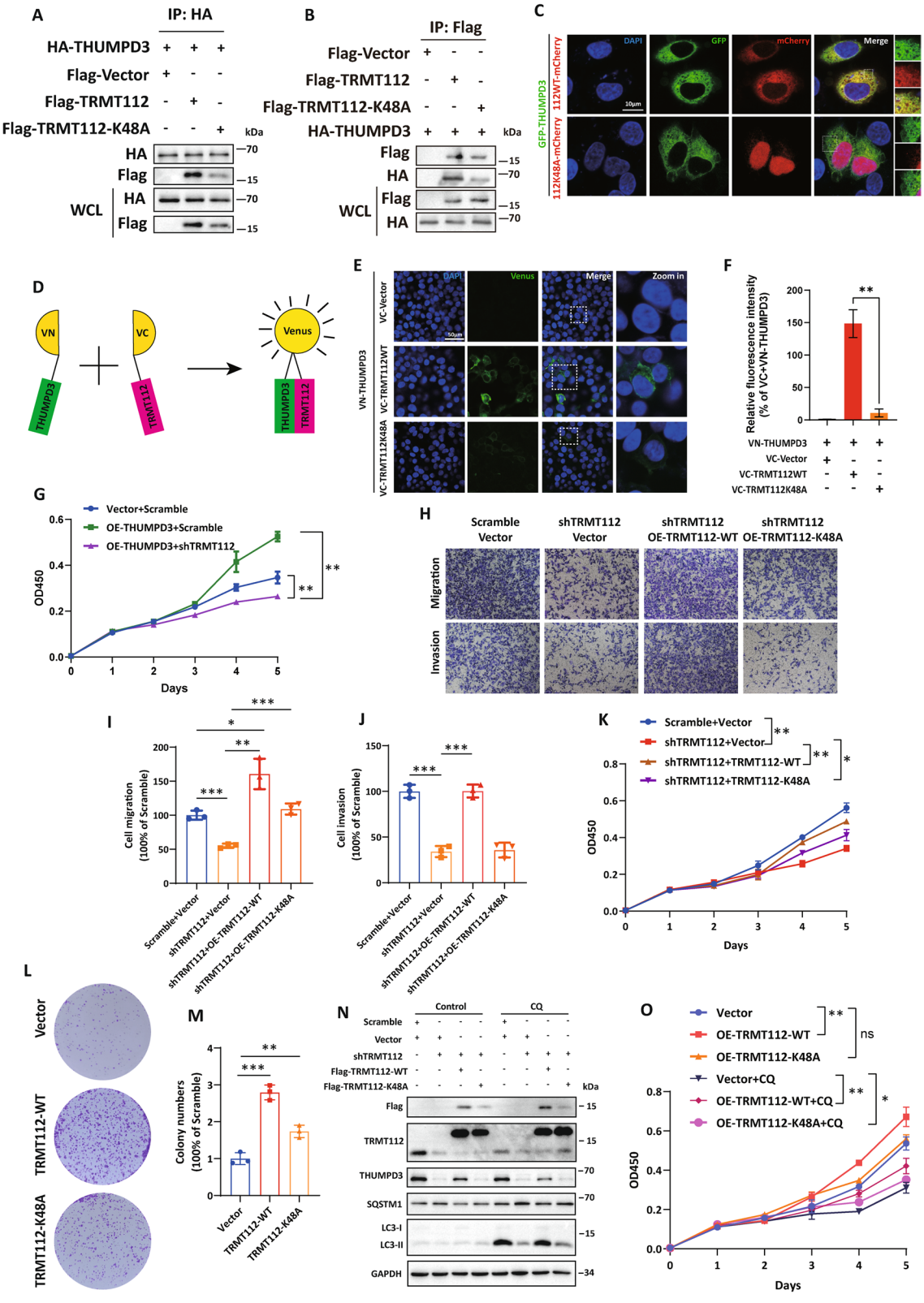

Fig. 5 (See legend on next page.)

(See figure on previous page.)

Fig. 5 The interaction of THUMPD3 with TRMT112 is critical for the maintenance of pancreatic cancer cell growth and autophagy. **A**, **B** Analysis of the interaction between exogenous HA-THUMPD3 and Flag-TRMT112 (WT or K48A mutation) in HEK-293T cells by co-immunoprecipitation (Co-IP) and reciprocal Co-IP. Protein interactions were assessed by western blotting. **C** The co-localization of mCherry-tagged TRMT112 WT or K48A and EGFP-tagged THUMPD3 in HeLa cells were analyzed with confocal microscopy. **D** The underlying principle of BiFC is the refolding and maturation of a chromophore that occurs upon the interaction of THUMPD3 and TRMT112 bearing complementary fragments of the Venus protein. **E** Subcellular localization of the BiFC THUMPD3-TRMT112 interaction. HEK-293T cells grown on glass coverslips were transfected with the BiFC VC-TRMT112 WT or K48A/VN-THUMPD3 combination and VC-vector/VN-THUMPD3, respectively. BiFC analyzed by confocal microscopy. **F** The fluorescence intensity of BiFC was quantified ($n=3$). **G** MTT assay for PANC-1 cells were transfected vector or THUMPD3 with or without TRMT112 knockdown ($n=5$). **H-J** Representative images and quantification of the transwell assays with or without matrigel of PANC-1 cells stably expressed Scramble RNA or TRMT112 shRNA and re-expression TRMT112 WT or K48A ($n=3$). **K** MTT assay for PANC-1 cells were stably expressed Scramble RNA or TRMT112 shRNA and re-expression TRMT112 WT or K48A ($n=5$). **L, M** Representative images and quantification of the plate colony formation assays of PANC-1 cells were stably expressed Scramble RNA or TRMT112 shRNA and re-expression TRMT112 WT or K48A ($n=3$). **N** PANC-1 cells were stably expressed with Scramble RNA or TRMT112 shRNA and re-expression TRMT112 WT or K48A; the cells were then treated with or without CQ (20 μM) treatment for another 6 h. Then, the cell lysates were sent to western blotting using indicated antibodies. **O** MTT assay for PANC-1 cells were stably expressed TRMT112 WT or K48A; the cells were then treated with or without CQ (20 μM) treatment for indicated duration ($n=5$). *$p<0.05$; **$p<0.01$; ***$p<0.001$. Data were presented as mean ± SD

PANC-1 cells, supporting that TFEB acts downstream of the THUMPD3-TRMT112 complex. Consistently, immunohistochemical analysis of xenograft tumors showed that knockdown of THUMPD3 or TRMT112 significantly reduced TFEB expression (Fig. S9E and S9F), further supporting the regulatory relationship between the THUMPD3-TRMT112 complex and TFEB in vivo. Furthermore, analysis of the TCGA-PAAD cohort confirmed significant positive correlations between the expression of THUMPD3-TRMT112 and several key autophagy-related genes coordinately controlled by TFEB (Fig. S10A), reinforcing the clinical relevance of this regulatory relationship.

Given the established role of tRNA modification in translation regulation, we next investigated whether THUMPD3/TRMT112 influences TFEB expression at the translational level. Puromycin incorporation assays showed that global protein synthesis was significantly inhibited upon depletion of THUMPD3 or TRMT112 in PANC-1 and AsPC-1 cells (Fig. 6G). Specifically, knockdown of THUMPD3 or TRMT112 markedly reduced TFEB protein levels, an effect that was further exacerbated by the transcriptional inhibitor Actinomycin D (Fig. 6H). These results indicate that THUMPD3 and TRMT112 regulate TFEB primarily at the translational level, rather than by affecting its transcription. In summary, we reveal that the THUMPD3-TRMT112 complex promotes pancreatic cancer cell proliferation and autophagy by enhancing TFEB protein translation, thereby increasing the transcriptional activation of autophagy-related target genes.

THUMPD3-TRMT112 mediated $tRNA^{Leu(CAG)}$ m^2G modification promotes TEFB translation level in pancreatic cancer cells

The THUMPD3-TRMT112 complex has been demonstrated to play a crucial role in the m^2G modification of tRNA [23]. Bioinformatic analysis of the amino acid sequence revealed that Leu exhibits the highest abundance in autophagy-related protein sequences (Fig. 7A). Subsequent RSCU analysis of codons corresponding to m^2G-modified tRNAs demonstrated high occupancy of Leu (CAG) codons in TFEB and ULK1 transcripts (Fig. 7B). Given TFEB's role in broadly regulating autophagy-related gene transcription, these findings suggest that Leu (CAG) translation efficiency is critical for TFEB protein level. To evaluate the impact of THUMPD3 and TRMT112 knockdown on the translation efficiency of 6 × Leu (CTG) and TFEB, we constructed luciferase reporters containing either 6 × Leu (CTG) repeats or TFEB coding sequences (Fig. 7C). Both the 6 × Leu (CTG) repeat and TFEB CDS showed significantly reduced translation efficiency upon THUMPD3 orTRMT112 knockdown (Fig. 7D and E). To further validate the functionality of $tRNA^{Leu(CAG)}$ in pancreatic cancer cells, we generated a stable PANC-1 cell line expressing $tRNA^{Leu(CAG)}$ (Fig. S11A). Notably, overexpression of $tRNA^{Leu(CAG)}$ alone did not significantly increase TFEB protein levels, whereas co-expression with THUMPD3 substantially augmented TFEB translation (Fig. 7F). This indicates that both the abundance of the $tRNA^{Leu(CAG)}$ and its m^2G modification by the THUMPD3-TRMT112 complex are required for efficient TFEB synthesis.

Consistent with the role of m^2G modifications in tRNA stability, LC–MS analysis confirmed that THUMPD3 knockdown significantly decreased global m^2G levels in tRNAs (Fig. 7G and H). Consequently, quantitative RT-qPCR revealed a specific reduction in mature $tRNA^{Leu(CAG)}$ levels (Fig. 7I), indicating that THUMPD3-TRMT112 complex controls $tRNA^{Leu(CAG)}$ abundance indirectly by maintaining its m^2G methylation and stability, rather than directly regulating its transcription. Despite its inability to significantly elevate TFEB protein alone, overexpression of $tRNA^{Leu(CAG)}$ was sufficient to enhance autophagy (Fig. 7J) and promote cell proliferation (Fig. 7K). This suggests that increased $tRNA^{Leu(CAG)}$ abundance can influence these processes through alternative mechanisms, such as the generation of tRNA-derived fragments known to regulate signaling pathways,

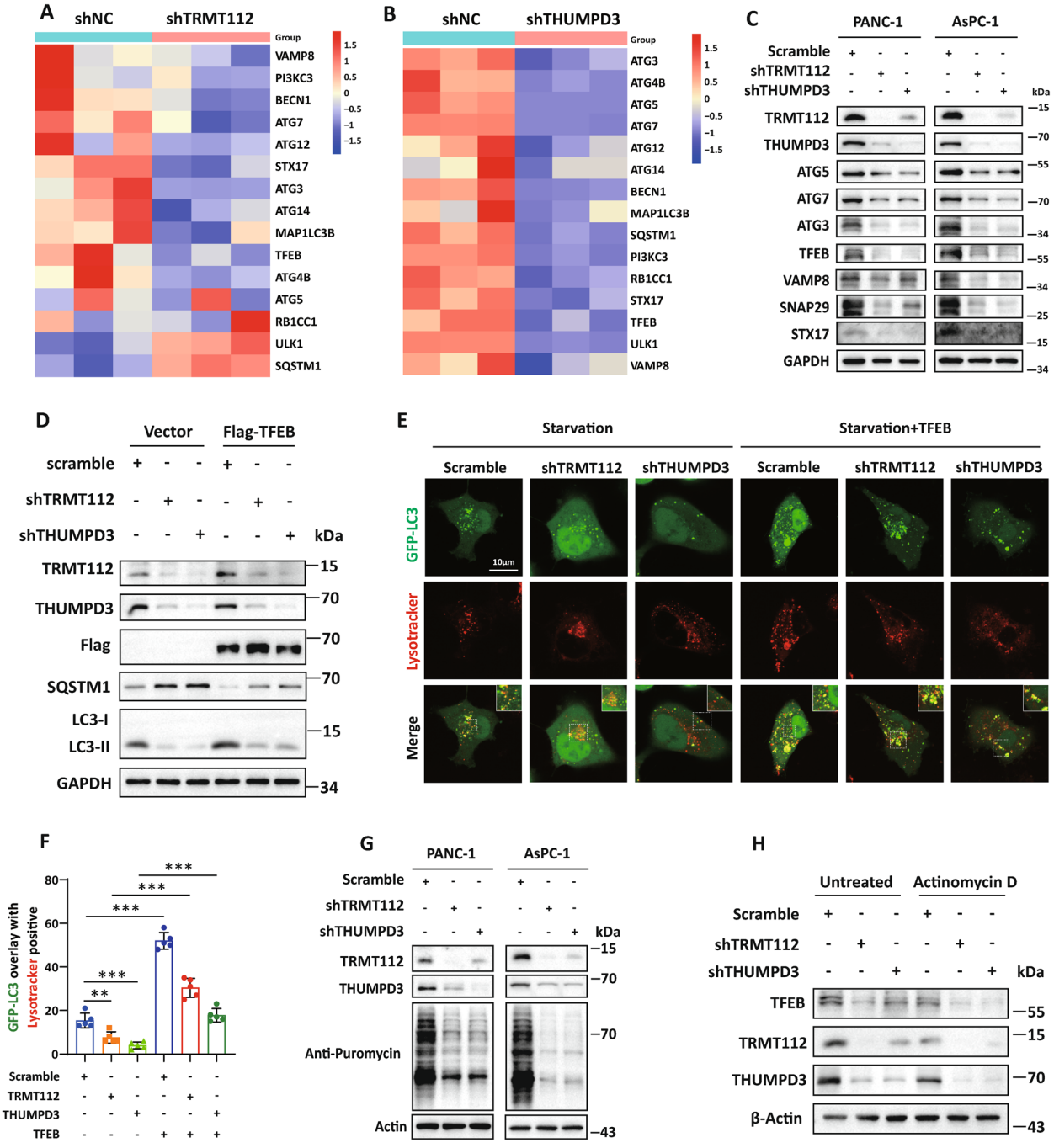

Fig. 6 TFEB is a potential downstream regulator of THUMPD3-TRMT112 mediating pancreatic cancer cell growth and autophagy. **A**, **B** The expression of autophagy related gene mRNAs in PANC-1 cells were stably expressed with Scramble RNA, THUMPD3 or TRMT112 shRNA and then assessed by qRT-PCR ($n=3$). **C** The whole cell lysates of PANC-1 and ASPC-1 cells were stably expressed with Scramble RNA, THUMPD3 or TRMT112 shRNA and then analyzed by western blotting using the indicated antibodies. **D** PANC-1 cells were stably expressed with Scramble RNA, THUMPD3 or TRMT112 shRNA then infected with or without Flag-tagged TFEB by lentivirus. Then, the cell lysates were sent to western blotting using indicated antibodies. **E**, **F** Autophagosome fusion with lysosomes was detected by Lysotracker staining in PANC-1 cells. The PANC-1 cells were stably expressed with Scramble RNA, THUMPD3 or TRMT112 shRNA and transfected with GFP-LC3 or co-transfected Flag-TFEB and GFP-LC3 construct after 48 h were incubated with LysoTracker for 30 min for live imaging. And the percentage of GFP-LC3 puncta co-localizing with LysoTracker was quantified ($n=5$). **G** Global translation of PANC-1 and AsPC-1 cells with overexpression of Scramble RNA, THUMPD3 or TRMT112 shRNA. **H** PANC-1 cells were stably expressed with Scramble RNA, THUMPD3 or TRMT112 shRNA then treated with or without Actinomycin D (10 μM, 24 h). Then, the cell lysates were sent to western blotting using indicated antibodies. *$p<0.05$; **$p<0.01$; ***$p<0.001$. Data were presented as mean ± SD

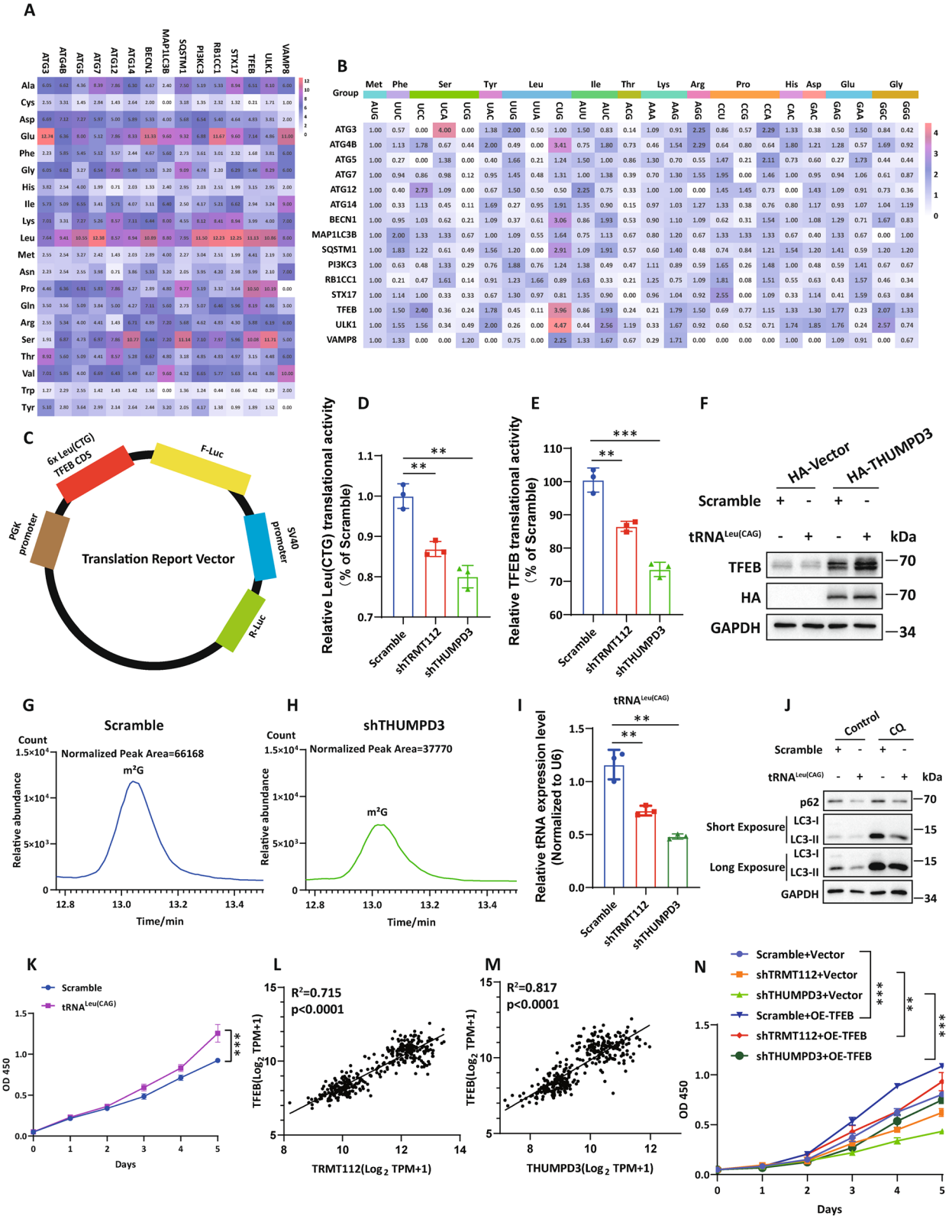

Fig. 7 (See legend on next page.)

(See figure on previous page.)

Fig. 7 THUMPD3-TRMT112 leads to TFEB translational changes. **A** Amino acid composition analysis of the autophagy related protein sequence. **B** RSCU analysis of the occupancy rate of m^2G-modified tRNA in autophagy-related genes. **C** Schematic representation of 6 × Leu(CTG) and TFEB CDS luciferase reporter vector generation. **D** Luciferase activity was measured in lysates of HEK-293 T cells transfected with 6 × Leu(CTG) luciferase constructs and Scramble RNA, THUMPD3 or TRMT112 shRNA. The luciferase activity was normalized to renilla luciferase activity ($n = 3$). **E** Luciferase activity was measured in lysates of HEK-293 T cells transfected with TFEB luciferase constructs and Scramble RNA, THUMPD3 or TRMT112 shRNA. The luciferase activity was normalized to renilla luciferase activity ($n = 3$). **F** PANC-1 cells were stably expressed with Vector, $tRNA^{Leu(CAG)}$ then infected with or without HA-tagged THUMPD3 by lentivirus. Then, the cell lysates were sent to western blotting using indicated antibodies. **G**, **H** LC-MS analysis of m^2G modification in total tRNA from PANC-1 cells expressing Scramble RNA or THUMPD3 shRNA. **I** The expression of $tRNA^{Leu(CAG)}$ in PANC-1 cells were stably expressed with Scramble RNA, THUMPD3 or TRMT112 shRNA and then assessed by qRT-PCR ($n = 3$). **J** PANC-1 cells were stably expressed with Scramble RNA, $tRNA^{Leu\ (CAG)}$ with or without CQ (20 μM) treatment for another 6 h. Then, the cell lysates were sent to western blotting using indicated antibodies. **K** MTT assay for PANC-1 cells were stably expressed with Vectoror $tRNA^{Leu(CAG)}$ ($n = 5$). **L**, **M** TFEB levels were positively correlated with the levels of THUMPD3 and TRMT112 in TCGA PAAD database. **N** MTT assay for PANC-1 cells were stably expressed with Scramble RNA or TRMT112 shRNA and re-expression vector or TFEB ($n = 5$). $^*p < 0.05$; $^{**}p < 0.01$; $^{***}p < 0.001$. Data were presented as mean ± SD

independent of elevating canonical TFEB translation (Fig. 8).

In an attempt to directly assess the dependency on THUMPD3-TRMT112-mediated methylation, we employed the pan-methylation inhibitor cycloleucine. This treatment resulted in a dissociative phenotype characterized by reduced TFEB protein levels and translation, alongside a concurrent activation of autophagy (Fig. S12A-C). This paradoxical induction of autophagy despite impaired TFEB synthesis suggests that cycloleucine may trigger compensatory stress responses, such as amino acid starvation pathways, that activate autophagy through alternative mechanisms [27]. This multifaceted and non-specific action starkly contrasts with the specific autophagy impairment seen with THUMPD3 orTRMT112 knockdown, highlighting the limitation of using broad methylation inhibitors and underscoring the need for tools that specifically target THUMPD3-TRMT112 complex or tRNA m^2G modification.

Moreover, we conducted an analysis of THUMPD3, TRMT112, and TFEB expression in pancreatic cancer patients from the TCGA database and observed a significant positive correlation among these three factors (Fig. 7L and M). We further performed H-score correlation analysis on IHC staining of *Thumpd3*, *Trmt112*, and *Tfeb* in the KPC mice pancreatic tissue, which demonstrated significant positive correlations across all three proteins within the tumors (Fig. S13A and S13B). Functionally, TFEB exhibited oncogenic properties and its expression rescued the growth inhibition induced by THUMPD3-TRMT112 knockdown (Fig. 7N). To further assess whether TFEB activity contributes to the proliferative effects of the THUMPD3-TRMT112 complex, we treated PANC-1 cells overexpressing THUMPD3 or TRMT112 with the TFEB transcriptional inhibitor Eltrombopag. Eltrombopag substantially reduced the proliferation advantage induced by THUMPD3 or TRMT112 overexpression (Fig. S14A). Overall, our data demonstrate that the THUMPD3-TRMT112 complex promotes TFEB translation by mediating m^2G modification of $tRNA^{Leu(CAG)}$, which in turn stabilizes the tRNA. This mechanism is essential for sustaining the autophagic and proliferative capacity of pancreatic cancer cells.

Discussion

The THUMPD3-TRMT112 complex catalyzes m^2G tRNA modification, with TRMT112 acting as a critical cofactor that stabilizes THUMPD3 and enhances its catalytic activity. Although loss of THUMPD3 has been shown to impair cell proliferation and TRMT112 has been proposed as a potential oncogene, the precise role of this complex and its associated tRNA m^2G modification in tumorigenesis has not been fully defined [23, 24, 28]. Here, we define a previously unrecognized regulatory axis in pancreatic cancer, linking tRNA m^2G modification to autophagy through translational regulation. We demonstrate that the THUMPD3-TRMT112 complex is significantly upregulated in human pancreatic cancer and genetically engineered KPC mice models, with higher expression levels correlating with poorer patient prognosis. Functionally, we established that THUMPD3-TRMT112-mediated m^2G tRNA modification is critical for pancreatic cancer growth, as its knockdown suppressed tumor progression in part by regulating autophagic flux via a translational control mechanism(Fig .8).

THUMPD3-TRMT112 can mediate m^2G modification on multiple tRNAs [23]. To elucidate the underlying mechanism, we found that THUMPD3-TRMT112 can specifically modify $tRNA^{Leu(CAG)}$, thereby enhancing the translational efficiency of TFEB mRNA. TFEB, a transcription factor central to the regulation of autophagy and lysosomal biogenesis, requires efficient translation to sustain the elevated autophagic activity characteristic of pancreatic cancer cells [7]. Consistently, depletion of THUMPD3-TRMT112 reduced the availability of m^2G-modified $tRNA^{Leu(CAG)}$, thereby impairing TFEB translation, disrupting autophagy, and inhibiting tumor growth. These findings reveal a previously unrecognized link between tRNA modification and autophagy regulation in pancreatic cancer, highlighting the contribution of post-transcriptional mechanisms to tumor maintenance.

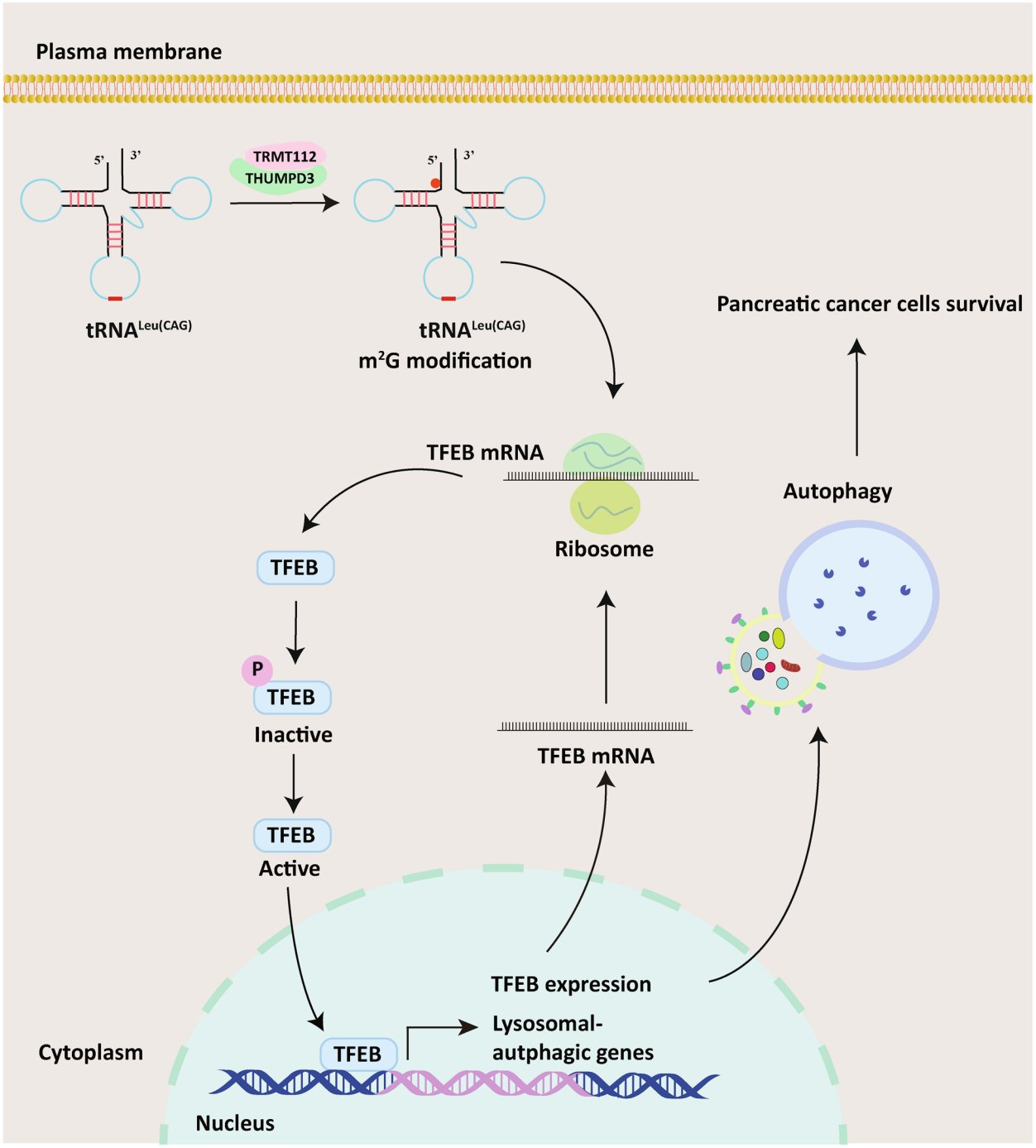

Fig. 8 The proposed mechanism by which THUMPD3-TRMT112 facilitates the progression of pancreatic cancer by augmenting TFEB translation via tRNA$^{Leu(CAG)}$

The functional importance of the THUMPD3-TRMT112 interaction was further supported by our analysis of the TRMT112-K48A mutant [24]. This mutation disrupted the binding interface between THUMPD3 and TRMT112, led to aberrant nuclear localization of TRMT112, and failed to restore autophagy, underscoring the requirement for an intact complex to ensure proper localization and function. Notably, the K48A mutant retained a residual ability to promote cancer cell proliferation despite its inability to sustain autophagy, indicating that TRMT112 also can contribute to tumor growth through autophagy-independent mechanisms. Based on these findings, the THUMPD3-TRMT112 complex emerges as a potential therapeutic target. Possible

strategies include the development of small-molecule inhibitors that interfere with the protein–protein interaction or enzymatic activity, RNA-based approaches to modulate expression, and inhibitory peptide designed to specifically block THUMPD3-TRMT112 binding [29–32]. Furthermore, given the established role of autophagy in mediating chemoresistance, inhibition of THUMPD3-TRMT112 may be explored in combination with conventional chemotherapy or clinically available autophagy inhibitors, such as hydroxychloroquine, to improve treatment efficacy. The observed association between THUMPD3-TRMT112 expression and patient outcome also suggests that this complex could serve as a prognostic biomarker to aid patient stratification.

Nevertheless, certain limitations of this study should be acknowledged. First, in the KPC mouse model, the assessment of the spatial relationship between Thumpd3-Trmt112 and autophagy markers was performed using serial tissue sections. While this approach demonstrates regional co-distribution at the tissue level, it does not permit definitive conclusions regarding single-cell co-localization. While our work focused on $tRNA^{Leu(CAG)}$ and its role in TFEB translation, it is likely that THUMPD3-TRMT112 modifies additional tRNAs that may contribute to tumor progression by regulating other oncogenes. Moreover, current methodological limitations in the quantitative detection of specifically tRNA modifications hinder a comprehensive assessment of the m^2G modification landscape in pancreatic cancer. Addressing these challenges and developing specific inhibitors will be critical for validating the therapeutic potential of targeting THUMPD3-TRMT112 complex.

In summary, this study identifies a novel mechanism by which THUMPD3-TRMT112-mediated tRNA m^2G modification contributes to pancreatic cancer progression through regulation of TFEB translation and autophagy. Our work establishes a conceptually new tRNA modification-autophagy regulatory circuit, positioning the THUMPD3-TRMT112 complex as a key node in pancreatic cancer and a compelling therapeutic target. Moreover, because THUMPD3-TRMT112 expression is predominantly localized to the epithelial compartment of PDAC, therapeutic strategies targeting THUMPD3-TRMT112 complex are expected to act primarily on tumor cells, providing focused antitumor activity with potentially reduced systemic toxicity. These findings provide a rationale for further investigation of the THUMPD3-TRMT112 complex as a therapeutic target and lay the groundwork for the development of new strategies, including RNA-based therapies, small-molecule inhibitors, peptide blockers, and rational combinatorial approaches with chemotherapy, to improve the management of pancreatic cancer.

Materials and methods

Cell lines, reagents, and antibodies

HEK-293 T cells, HeLa cells, Human pancreatic cancer cell lines PANC-1 and AsPC-1 were purchased from the cell center of Institute of Biochemistry and Cell Biology, Chinese Academy of Sciences. All cell lines were confirmed contamination-free by mycoplasma PCR testing and STR profiling. Autophagy inhibitor chloroquine diphosphate salt (CQ) was purchased from Sangon Biotech (Shanghai, A506569), Transcription inhibitor Actinomycin D was purchased from MedChemExpress(USA, HY-17559). EBSS (Servicebio, G4214) starvation in this study was carried out to switch the culture medium from the complete medium to the EBSS medium unless described otherwise. Commercially available antibodies used are as follows: anti-TRMT112 (ZENBIO, 864,221), anti-THUMPD3 (Proteintech, 19,807–1-AP), anti-GAPDH (Proteintech, 60,004–1-Ig), anti-Actin (Proteintech, 81,115–1-RR), anti-LC3 (Proteintech, 14,600–1-AP), anti-SQSTM1(Proteintech, 18,420–1-AP), anti-mouse HA (EMD Millipore, M180-3), anti-Rabbit HA (Proteintech, 51,064–2-AP), anti-mouse DDDDK(MBL,M185-3S), anti-mouse DDDDK(MBL,PM020), anti-ATG5 (Cell signaling technology,12,994), anti-ATG3 (Cell signaling technology,3415), anti-ATG7 (Cell signaling technology,8558), anti-TFEB (Proteintech,13,372–1-AP), anti-VAMP8 (Proteintech, 15,546–1-AP), anti-STX17 (ABclonal, A17174), anti-SNAP29 (ABclonal, A4290).

Plasmids construction, cell culture and transfection

DNA fragments encoding TRMT112 and THUMPD3 amplified by PCR from the cDNA obtained from HEK-293 T cells and cloned into pcDNA3.0–3 × HA (Miaolingbio, P9394), pCMV-3 × Flag (Sigma, E4401), pEGFP-C1(Miaolingbio, P0134) and pmCherry-N1(Miaolingbio, P0475), ptfLC3 (Mammalian expression of rat LC3 fused to mRFP and GFP) was a gift from Tamotsu Yoshimori (Addgene, 21,074). To overexpress individual tRNAs, we referred to the method of Esteban A et al. [33] and removed the pLKO.1 U6 promoter and cloned the tRNA genome sequence (including ~ 300 nt upstream and ~ 100 nt downstream) into the pLKO-ΔU6 vector. PANC-1, AsPC-1, HeLa and HEK-293 T cells were cultured in Dulbecco's modified Eagle's medium (DMEM; Servicebio, G4510). HeLa and HEK-293 T cells were treated with Lipofectamine 3000 followed by transfection with plasmids according to the experiment design.

Lentiviral production and creation of stable cell lines

The lentiviral vector pLKO.1-Neo (Miaolingbio, P33186) was utilized for subcloning shTRMT112 (#1 was 5′-AAC UUCGUGGCGCGUAUGAUA-3′, #2 was 5′-CGAAUU

CUGCCGUGUGUAU-3′), shTHUMPD3(#1 was 5′-AG AGACCGUGGCAAGAUAUAU-3′, #2 was 5′-GAGUC UCCACCGAAGAAAUAU-3′), and scramble RNA(5′-C ACCGACGGAGACAAAGCUUU –3′. Lentiviral vector pCDH-CMV-MCS-EF1-turboRFP-T2A-puro, a generous gift from Dr. Xiaorong Zhang (Institute of Biophysics, Chinese Academy of Sciences, China), was employed to subclone DNA fragments encoding TRMT112, TRMT112-K48A, THUMPD3 and TFEB. Co-transfection of 5 μg lentiviral constructs with viral packaging plasmids psPAX2 (3 μg) and pMD2.G (3 μg), also provided by Dr. Xiaorong Zhang, was performed in HEK-293 T cells cultured in 10 cm dishes. After replacing the medium with complete DMEM at 8 h post-transfection, the viral supernatant was collected at 48 h post-transfection and filtered through a 0.22 μm membrane. Subsequently, PANC-1 and AsPC-1 cells were exposed to the viral supernatant along with polybrene (Beyotime C0351) at a concentration of 10 μg/μl for transduction purposes. Selection for puromycin and/or G418 resistance commenced after 48 h of transfection initiation. The selection media were periodically changed every 3–4 days over several weeks to isolate and expand clones consisting of puromycin and/or G418-resistant cells for further characterization purposes. To maintain stable cell lines obtained from this process, a complete culture medium supplemented with puromycin (2 μg/ml) and/or G418 (100 μg/ml) was used.

Animal experiments

All animal experiments were conducted in accordance with a laboratory animal protocol approved by the Animal Care and Use Committee of Hubei University of Technology (HBUTXM20240113). Female BALB/c nude mice, aged four weeks and weighing between 18–22 g, were obtained from Hunan SJA laboratory animal (Changsha, China). C57BL/6N.129Cya-Krastm1 (LSL-G12D) Trp53tm1(LSL-R172H) Tg (Pdx1-Cre) (KPC) mice, aged four weeks and weighing between 18–22 g, were obtained from Cyagen Biosciences (China). For the shTHUMPD3 and shTRMT112 or CQ rescue xenograft model, PANC-1 cells (3×10^6) or (2×10^5) were injected subcutaneously into both sides of the back of five female BALB/c nude mice per group. After approximately two weeks, Autophagy inhibitor CQ was administered to the animals at a dose of 60 mg/kg body weight via intraperitoneal injection twice weekly. The dimensions (length and width) of the mouse xenograft tumors were measured every 5 days using calipers, and tumor volume (V) was calculated using the formula: V = [(length × width × width)/2]. At the end of the observation period, experimental mice were humanely euthanized and their tumors were surgically removed and weighed. For the pancreatic diseased tissue assay in KPC mice, the KPC mice were monitored until the development of ascites was observed. Subsequently, the mice were euthanized, and the diseased pancreatic tissue was surgically excised. The excised pancreatic diseased tissues were fixed in 4% paraformaldehyde at room temperature for 24 h. Immunohistochemical staining was then performed on the fixed tissues.

Immunohistochemistry

The paraffin sections were sequentially treated with 100% xylene, 95% alcohol, 90% alcohol, 80% alcohol, and 70% alcohol for deparaffinization. Subsequently, rehydration was carried out for a duration of 10 min. To inhibit endogenous peroxide activity, hydrogen peroxide (0.3% v/v) was applied. The antigen site was exposed by subjecting the samples to microwave heating in citrate buffer (pH 6.0) at a concentration of 15 μM for a period of 3 min. Non-specific antibody binding was reduced by incubating the glioma tissue sections with normal goat serum. primary antibody was then added to the sections while rabbit immunoglobulin (1:500 dilution) served as a negative control. Antibody staining occurred through overnight incubation at a temperature of 4 °C with gentle shaking. Following this step, the samples were subjected to biotinylated secondary goat anti-rabbit serum immunoglobulin G (IgG) antibody at a temperature of 37 °C for 30 min. After washing, the paraffin sections underwent incubation with streptavidin-avidin-conjugated horseradish peroxidase for 30 min. Hematoxylin counterstaining lasted for 30 min, and the paraffin sections were dehydrated in ethanol before mounting. Finally, the estimation of staining in tissue sections was conducted based on the H-score methodology.

Trans-well assay

For migration, stably overexpress PANC-1 and AsPC-1 cells was seeded in upper transwell chamber (Corning Incorporated, Corning, NY, USA) with 1×10^5 cells in 100uL of FBS-free medium. For invasion, transwell chamber pre-covered with Matrigel (Corning Incorporated, Corning, NY, USA) was used. Meanwhile, 500μL of medium containing 20% FBS was added to the lower cavity. 24 h later, the cells were fixed by 0.1% crystal violet and stained by 4% PFA Fix Solution. Under microscope, the number of invasive cells from 3 fields was counted.

Puromycin intake assay

Cells were incubated with medium containing 2.5 μg/mL puromycin for 30 min at 37 °C, and then subjected to protein isolation and western blotting. Anti-puromycin antibody (MABE343, Millipore, 1:20,000 dilution) was used to detect the new protein synthesis rate.

Transmission electron microscopy (TEM)

PANC-1 cells were knocked down with TRMT112 or THUMPD3 and fixed in 2.5% glutaraldehyde without washing at 37 °C and further fixed with 2% osmium tetroxide buffer. Then, the fixed cells were dehydrated using a graded ethanol series and embedded in Epon. Electron microscopy was performed with a HT7800 TEM transmission electron microscope (HITACHI, Japan).

Colony formation assay

PANC-1 and AsPC-1 human pancreatic cancer cells knocked down with TRMT112 or THUMPD3 were seeded into a 12-well plate and incubated with complete medium at 37 °C for 2–3 weeks. Then, the cells were fixed with 4% paraformaldehyde and stained with 2% crystal violet. Images were obtained and the number of colonies was counted.

Western blotting assay

Cell lysates or immunoprecipitates were heated in 1 × SDS loading buffer for 15 min at 98 °C. Proteins were separated by SDS-PAGE gels and transferred to 0.22 μm polyvinylidene fluoride (PVDF) membranes (Millipore, IPFL85R). After the PVDF membranes had been blocked with TBS-T containing 5% skimmed milk at room temperature for 2 h and incubated with primary antibodies and secondary antibodies, the protein signals in the PVDF membranes were detected using SuperPico ECL Chemiluminescence Kit (Vazyme, E422-02) according to the manufacturer's instructions.

Dual-luciferase reporter assay

To evaluate the regulatory impact of THUMPD3/TRMT112 on TFEB and Leu translation efficacy, a dual-luciferase reporter assay was conducted. The method proposed by Fange et al. [34]. is referenced in this study. Synthetic constructs of 6 × Leu (CTG) and TFEB CDS were obtained from Sangon Biotech and inserted upstream of the luciferase (Firefly) gene in the pmiR-GLO dual-luciferase vector (Promega, E1330). HEK293T cells were co-transfected with luciferase reporter plasmids along with either THUMPD3/TRMT112 shRNA or scramble RNA using Lipofectamine 3000. Following a transfection period of 48 h, the luminescence ratio between the experimental reporter (Firefly) and control reporter (Renilla) was determined. All experiments were performed in triplicate.

Immunoprecipitation

Cells were washed twice with phosphate-buffered saline (PBS; Servicebio, WGSH30256-01) and lysed with RIPA lysis buffer (50 mM Tris–HCl pH 7.4, 150 mM NaCl, 1% Triton X-100 [Sangon Biotech, 9002–93-1], 10 mM NaF, and 1 mM EDTA) containing proteinase inhibitor cocktail (Biomake, B14001). Protein concentration was measured using an Enhanced BCA Protein Assay Kit (Beyotime, P0009). Cell lysates were incubated overnight with primary antibodies according to each individual experiment after pretreatment with IgG and protein A/G magic beads (Bimake, B23202), and then incubated with protein A/G magic beads for 2 h at 4 °C. The beads were spun down and washed five or six times, and followed by western blotting assay.

Bimolecular fluorescence complementation assay

Paired cVenus-TRMT112 and nVenus-THUMPD3 constructs were co-transfected in HEK-293 T for 48 h. Venus signals were then detected with a confocal laser-scanning microscope (Leica SP8, Wetzlar, Germany) at 488 nm.

MTT assay

Human pancreatic cancer PANC-1 and AsPC-1 cells (1×10^3 cells/well) knocked down with THUMPD3 and TRMT112 were seeded into 96-well plates, then cells were stained at the indicated time points with 100 μl sterile MTT dye (0.5 mg/ml; Solarbio, M8180) for 4 h at 37 °C. After adding 150 μL DMSO (Biosharp, BS186), the number of viable cells was assessed by measurement of the absorbance at 450 nm by a microplate reader. All experiments were performed in triplicate.

RNA extraction and real-time PCR

Total RNA was isolated from cells using TRIzol reagent (Invirogen) according to the manufacturer's protocol. RNAs were quantified using a NanoDrop One instrument (ThermoFisher). cDNA was reverse transcribed using a HiScript cDNA synthesis kit (Vazyme, R323–01). For gene expression analysis, real-time PCR was performed using a QuantStudio 3 instrument (Thermo, USA) and Hieff qPCR SYBR Green Master Mix (YEASEN, 11202ES08). As an internal control, β-actin was used. The sequences of the primers used in real-time PCR were shown in Table 1. For tRNA expression analysis, we referred to the method of Tsuyoshi et al. [35]. for reverse transcription and specific tRNA primer design.

tRNA isolation, digestion and LC–MS analysis

tRNA was isolated from total RNA samples by Urea-PAGE electrophoresis. 60-90nt band of tRNA was excised and purified by ethanol precipitation. Purified tRNA was quantified using Qubit RNA HS Assay kit (ThermoFisher, Q32855). tRNA was hydrolysed to single nucleosides and then nucleosides were dephosphorylated by enzyme mix. Pretreated nucleosides solution was deproteinized using Satorius 10,000-Da MWCO spin filter. Analysis of nucleoside mixtures was performed on Agilent 6460 QQQ mass spectrometer with an Agilent 1260 HPLC system. Multi reaction monitoring (MRM) mode was performed

Table 1 Primers used in real-time PCR for autophagy gene

Primers	Forward (5′–3′)	Reverse (5′–3′)
ATG5	AGAAGCTGTTTCGTCCTGTG	AGGTGTTTCCAACATTGGCT
ATG7	TGGTTACAAGCTTGGCTGCT	TCAAGAACCTGGTGAGGCAC
BECN1	TCCGGGCTCCCGAGG	GGGGGATGAATCTGCGAGAG
VAMP8	AATGATCGTGTGCGGAACCT	ATTTCCGAGCCACCTTCTGC
STX17	TCGTGGGAAACCTTAGAAGCG	GCAGCACTGTTGACATGGTCG
ULK1	TGGCCCTGTACGACTTCC	CCTGATGGTGTCCTCGCT
ATG4B	TTGGAGGTGGACACAAAGG	GCGCTATCTGGTGAATGGA
ATG3	CCTACCAACAGGCAAACAA	CGCCATCACCATCATCTT
PIK3C3	CTTGCCAGTGAGAACATCC	GGGACCATACACATCCCA
ATG12	AGTGTTTTGGCAGTGATGG	GCTGTCTCTTCCGTGAAAAT
TFEB	GTGCCTGGGGAGGTGTT	TCTGATGCTGCGACTGCT
RB1CC1	AGAATGTTTGGGAAGACTGG	CTGACTTGGGAAATGAGGTT
MAP1LC3B	GACCCTGGAGAAAGAGTGG	TCCGTAACAACACAGGCA
SQSTM1	CCACTTTTGCCCACCTCT	CACCCTAACCCCTGATCCT
ATG14	TGAGAGACCCCGCAGAT	TCACAGACCCATCGTCCT
β-actin	TCACCCACACTGTGCCCATCTACGA	CAGCGGAACCGCTCATTGCCAATGG

because of its high selectivity and sensitivity attained working with parent-to-product ion transitions.

Tandem RFP-GFP-LC3 and LysoTracker staining

PANC-1 cells transfected with the appropriate plasmids were grown on 12-well plates, and for confocal microscopy on glass chambers, at 60% density and cultured for 48 h. After treatment with or without EBSS or CQ for 2 h, cells were fixed with 4% paraformaldehyde in PBS and permeabilized with 0.5% Triton X-100. DAPI (Solarbio, C0065) was used for nuclei staining. For Tandem RFP-GFP-LC3 assay, cells plated on the glass chambers. For live cell LysoTracker staining, PANC-1 cells transfected with the appropriate plasmids were grown on confocal dishes, and the cells were incubated for 30 min in cell culture medium with 10 μM LysoTracker Red (Yeasen, 40739ES50). The glass chambers or confocal dishes were examined with a confocal laser-scanning microscope (Leica SP8, Wetzlar, Germany) using a 63 × oil immersion objective. Data analysis was performed using the ImageJ software.

Statistical analysis

All experiments were performed independently at least three times. All statistical analysis was performed using GraphPad Prism 8.0 software (GraphPad, La Jolla, CA, USA). All data are presented as mean ± SD (standard deviation) from triplicates. $p < 0.05$ were statistically significant. For comparisons between two groups, statistical significance was determined by paired Student's t-test. For comparisons involving three or more groups, one-way ANOVA with Tukey's post hoc test was applied; *represents $p < 0.05$, **represents $p < 0.01$ and ***represents $p < 0.001$.

Supplementary Information

The online version contains supplementary material available at https://doi.org/10.1186/s12943-025-02540-2.

Supplementary Material 1.

Supplementary Material 2.

Acknowledgements

We also thank Hubei University of Technology and University of Alberta for financial support for this research.

Disclosure statement

No potential conflict of interest was reported by the authors.

Authors' contributions

WY, wrote the manuscript and performed molecular biology experiments. JT and CZ designed the whole project and supervised all experiments. WY, SL, YX, RT, YL, XC, RZ, HL, SX, DG, QZ, WQ and CY. conducted all experiments and analyzed the data.YZ and X-ZC provided support with experimental and clinical techniques. All authors read and approved the final manuscript.

Funding

We thank Hubei University of Technology for the research equipment and technical support for this research. This work was supported by the National Natural Science Foundation of China (32571378 and 32270768 to CFZ, 82273970 and U25A20650 to JFT, 82370715 to XZC), the National Key R&D Program of China (2023YFC2507900 to JFT), the Innovation Group Project of Hubei Province (2023AFA026 to JFT). The Key Cultivation Project of Hubei Province for Science and Technology (2024DJA037 to JFT). The National Natural Science Foundation of Hubei (2025AFA085 to CFZ).

Data availability

The data that support the findings of this study are available from the corresponding author upon reasonable request.

Declarations

Ethics approval and consent to participate

Not applicable.

Consent for publication

All authors consent to publication.

Competing interests

The authors declare no competing interests.

Received: 20 May 2025 / Accepted: 28 November 2025
Published online: 13 January 2026

References

1. Cai J, Chen H, Lu M, Zhang Y, Lu B, You L, et al. Advances in the epidemiology of pancreatic cancer: trends, risk factors, screening, and prognosis. Cancer Lett. 2021;520:1–11.
2. Siegel RL, Miller KD, Fuchs HE, Jemal A. Cancer statistics, 2021. CA Cancer J Clin. 2021;71:7–33.
3. Klein AP. Pancreatic cancer epidemiology: understanding the role of lifestyle and inherited risk factors. Nat Rev Gastroenterol Hepatol. 2021;18:493–502.
4. Yuan W, Fang W, Zhang R, Lyu H, Xiao S, Guo D, et al. Therapeutic strategies targeting AMPK-dependent autophagy in cancer cells. Biochim Biophys Acta Mol Cell Res. 2023;1870:119537.
5. Zhang R, Yang Y, He C, Zhang X, Torraca V, Wang S, et al. RUNDC1 inhibits autolysosome formation and survival of zebrafish via clasping ATG14-STX17-SNAP29 complex. Cell Death Differ. 2023;30:2231–48.
6. Yang A, Herter-Sprie G, Zhang H, Lin EY, Biancur D, Wang X, et al. Autophagy sustains pancreatic cancer growth through both cell-autonomous and nonautonomous mechanisms. Cancer Discov. 2018;8:276–87.

7. Tan A, Prasad R, Lee C, Jho EH. Past, present, and future perspectives of transcription factor EB (TFEB): mechanisms of regulation and association with disease. Cell Death Differ. 2022;29:1433–49.
8. Chen H, Gong S, Zhang H, Chen Y, Liu Y, Hao J, et al. From the regulatory mechanism of TFEB to its therapeutic implications. Cell Death Discov. 2024;10:84.
9. Seo JW, Choi J, Lee SY, Sung S, Yoo HJ, Kang MJ, et al. Autophagy is required for PDAC glutamine metabolism. Sci Rep. 2016;6:37594.
10. Klein K, Werner K, Teske C, Schenk M, Giese T, Weitz J, et al. Role of TFEB-driven autophagy regulation in pancreatic cancer treatment. Int J Oncol. 2016;49:164–72.
11. Kim JH, Lee J, Cho YR, Lee SY, Sung GJ, Shin DM, et al. TFEB supports pancreatic cancer growth through the transcriptional regulation of glutaminase. Cancers (Basel). 2021. https://doi.org/10.3390/cancers13030483.
12. Zhao B, Dierichs L, Gu JN, Trajkovic-Arsic M, Axel HR, Savvatakis K, et al. TFEB-mediated lysosomal biogenesis and lysosomal drug sequestration confer resistance to MEK inhibition in pancreatic cancer. Cell Death Discov. 2020;6:12.
13. Zhou C, Yi C, Yi Y, Qin W, Yan Y, Dong X, et al. LncRNA PVT1 promotes gemcitabine resistance of pancreatic cancer via activating Wnt/beta-catenin and autophagy pathway through modulating the miR-619-5p/Pygo2 and miR-619-5p/ATG14 axes. Mol Cancer. 2020;19:118.
14. Karasic TB, O'Hara MH, Loaiza-Bonilla A, Reiss KA, Teitelbaum UR, Borazanci E, et al. Effect of gemcitabine and nab-paclitaxel with or without hydroxychloroquine on patients with advanced pancreatic cancer: a phase 2 randomized clinical trial. JAMA Oncol. 2019;5:993–8.
15. Lin Y, Shi Q, Yang G, Shi F, Zhou Y, Wang T, et al. A small-molecule drug inhibits autophagy gene expression through the central regulator TFEB. Proc Natl Acad Sci USA. 2023;120:e2081297176.
16. Ren D, Mo Y, Yang M, Wang D, Wang Y, Yan Q, et al. Emerging roles of tRNA in cancer. Cancer Lett. 2023;563:216170.
17. Haruehanroengra P, Zheng YY, Zhou Y, Huang Y, Sheng J. RNA modifications and cancer. RNA Biol. 2020;17:1560–75.
18. Suzuki T. The expanding world of tRNA modifications and their disease relevance. Nat Rev Mol Cell Biol. 2021;22:375–92.
19. Hori H. Methylated nucleosides in tRNA and tRNA methyltransferases. Front Genet. 2014;5:144.
20. Orellana EA, Siegal E, Gregory RI. TRNA dysregulation and disease. Nat Rev Genet. 2022;23:651–64.
21. Pallan PS, Kreutz C, Bosio S, Micura R, Egli M. Effects of N2,N2-dimethylguanosine on RNA structure and stability: crystal structure of an RNA duplex with tandem m2 2G:a pairs. RNA. 2008;14:2125–35.
22. Wang C, Ulryck N, Herzel L, Pythoud N, Kleiber N, Guerineau V, et al. N 2-methylguanosine modifications on human tRNAs and snRNA U6 are important for cell proliferation, protein translation and pre-mRNA splicing. Nucleic Acids Res. 2023;51:7496–519.
23. Yang WQ, Xiong QP, Ge JY, Li H, Zhu WY, Nie Y, et al. THUMPD3-TRMT112 is a m2G methyltransferase working on a broad range of tRNA substrates. Nucleic Acids Res. 2021;49:11900–19.
24. Brumele B, Mutso M, Telanne L, Ounap K, Spunde K, Abroi A, et al. Human TRMT112-Methyltransferase Network Consists of Seven Partners Interacting with a Common Co-Factor. Int J Mol Sci 2021;22.
25. Han H, Yang C, Ma J, Zhang S, Zheng S, Ling R, et al. N(7)-methylguanosine tRNA modification promotes esophageal squamous cell carcinoma tumorigenesis via the RPTOR/ULK1/autophagy axis. Nat Commun. 2022;13:1478.
26. Zhou C, Liang Y, Zhou L, Yan Y, Liu N, Zhang R, et al. TSPAN1 promotes autophagy flux and mediates cooperation between WNT-CTNNB1 signaling and autophagy via the MIR454-FAM83a-TSPAN1 axis in pancreatic cancer. Autophagy. 2021;17:3175–95.
27. Huang W, Li N, Zhang Y, Wang X, Yin M, Lei QY. AHCYL1 senses SAH to inhibit autophagy through interaction with PIK3C3 in an MTORC1-independent manner. Autophagy. 2022;18:309–19.
28. Xu H, Jiang C, Yao F, Liang H, Yan H, Chen D, et al. Pan-cancer analysis reveals the relation between TRMT112 and tumor microenvironment. J Oncol. 2022;2022:1445932.
29. Yuan W, Zhang R, Lyu H, Xiao S, Guo D, Zhang Q, et al. Dysregulation of tRNA methylation in cancer: mechanisms and targeting therapeutic strategies. Cell Death Discov. 2024;10:327.
30. Zhou C, Zhu X, Liu N, Dong X, Zhang X, Huang H, et al. B-lymphoid tyrosine kinase-mediated FAM83a phosphorylation elevates pancreatic tumorigenesis through interacting with beta-catenin. Signal Transduct Target Ther. 2023;8:66.
31. Zhou C, Dong X, Li S, Xi Y, Liu Y, Qian X, et al. Serine/threonine/tyrosine kinase 1 drives pancreatic carcinogenesis via GSK3beta sequestration-mediated Wnt/beta-catenin pathway hyperactivation. Signal Transduct Target Ther. 2025;10:205.
32. Shi M, Zhang R, Lyu H, Xiao S, Guo D, Zhang Q, et al. Long non-coding RNAs: emerging regulators of invasion and metastasis in pancreatic cancer. J Adv Res. 2025. https://doi.org/10.1016/j.jare.2025.02.001.
33. Orellana EA, Liu Q, Yankova E, Pirouz M, De Braekeleer E, Zhang W, et al. METTL1-mediated m(7)G modification of Arg-TCT tRNA drives oncogenic transformation. Mol Cell. 2021;81:3323–38.
34. Liu F, Clark W, Luo G, Wang X, Fu Y, Wei J, et al. ALKBH1-mediated tRNA demethylation regulates translation. Cell. 2016;167:816–28.
35. Udagawa T, Seki M, Inada T. Optimized protocol for tRNA identification in the ribosomal complexes from human cell lines. STAR Protoc. 2021;2:100615.

Publisher's Note